Cellular Microbiology (2011) **13**(11), 1824–1837
doi:10.1111/j.1462-5822.2011.01664.x
First published online 14 September 2011

The bacterial lipopeptide surfactin targets the lipid fraction of the plant plasma membrane to trigger immune-related defence responses

Guillaume Henry,[1] Magali Deleu,[2] Emmanuel Jourdan,[1] Philippe Thonart[1] and Marc Ongena[1]*
[1]*Walloon Center for Industrial Biology and* [2]*Unité de Chimie Biologique Industrielle, University of Liège/Gembloux Agro-Bio Tech, 5030 Gembloux, Belgium.*

Summary

The lipopeptide surfactin secreted by plant-beneficial *bacilli* has crucial biological functions among which the ability to stimulate immune-related responses in host tissues. This phenomenon is important for biological control of plant diseases but its molecular basis is still poorly understood. In this work, we used various approaches to study the mechanism governing the perception of this biosurfactant at the plant cell surface. Combining data on oxidative burst induction in tobacco cells, structure/activity relationship, competitive inhibition, insertion kinetics within plant membranes and thermodynamic determination of binding parameters on model membranes globally indicates that surfactin perception relies on a lipid-driven process at the plasma membrane level. Such a sensor role of the lipid bilayer is quite uncommon considering that plant basal immunity is usually triggered upon recognition of microbial molecular patterns by high-affinity proteic receptors.

Introduction

In plants, the so-called basal immune response is activated by the perception of conserved molecular motifs typically harboured by microbial phytopathogens and referred to either as PAMPs (pathogen-associated molecular patterns) or more broadly as MAMPs (microbial-AMPs) (Boller and Felix, 2009; Nurnberger and Kemmerling, 2009). These elicitors are usually recognized by specific high-affinity pattern recognition receptors (PRR) located in the plant plasma membrane (Chinchilla *et al*., 2006; Boller and Felix, 2009; Kishimoto *et al*., 2010). These proteic receptors typically contain an extracellular ligand-binding domain with leucine-rich repeats (LRR), a single transmembrane domain and an intracellular serine/threonine kinase-signalling domain. They are referred to as receptor-like kinases (RLKs). Receptor-like proteins (RLPs) are similarly structured, but lack the cytoplasmic kinase domain. A large number of genes encoding RLKs and RLPs are transcriptionally induced upon PAMP treatment, illustrating the large diversity of such perception systems and suggesting their potential role in defence (Zipfel *et al*., 2004; 2006). The effector-receptor association activates a phosphorylation cascade and early defence-related events that may ultimately lead to pathogen restriction. Some successful invaders can overcome this pathogen-triggered immunity (PTI) through the delivery of effector proteins into host cells but plants also evolved to perceive these effectors by means of the products of specific disease resistance (*R*) genes. The major class of *R* genes encodes a nucleotide binding site (NBS) and a block of LRR (McHale *et al*., 2006). Generally, NBS-LRR proteins do not contain predicted transmembrane segments or signal peptides, suggesting they are soluble cytoplasmic proteins. NBS-LRR sequences subclassification is based on the N-terminal domain, which contains either a leucine zipper (LZ) motif (Lokossou *et al*., 2009) or a Toll and interleukin-1 receptors homology region (TIR) (Yang *et al*., 2010). Specific recognition of effectors by R proteins allows the host to mount a second layer of defence called effector-triggered immunity (ETI). ETI is generally associated with hypersensitive response (HR) and programmed cell death at the penetration site (Jones and Dangl, 2006). This *R* gene-mediated resistance is conceptually expressed through the same defence responses as those that are active in basal resistance, but differs in its kinetics and quantitative aspects (Boller and Felix, 2009).

Some non-pathogenic bacteria are also able to reduce plant disease through the stimulation of a primed state in the host plant allowing an accelerated activation of defence responses upon subsequent pathogen attacks (Conrath *et al*., 2006; Bakker *et al*., 2007). The localized

Received 20 May, 2011; revised 15 July, 2011; accepted 18 July, 2011. *For correspondence. E-mail Marc.Ongena@ulg.ac.be; Tel. (+32) 81622311; Fax (+32) 81614222.

perception of these beneficial isolates typically results in a resistant state that extends to all organs of the host plant (the induced systemic resistance, ISR). Driven by the evident potential for biological control of plant diseases in agriculture, fundamental as well as applied research on ISR has been tremendously boosted in the past decades. Various compounds with plant defence-eliciting properties were isolated from multiple genera such as *Pseudomonas*, *Serratia* and *Bacillus* (Ongena and Jacques, 2008). They can be cell surface components such as flagellin and lipopolysaccharides or secreted molecules (see De Vleesschauwer and Hofte, 2009 for a review) among which amphiphilic compounds with surfactant activity such as rhamnolipids (Vatsa *et al*., 2010), N-alkylated benzylamine (Ongena *et al*., 2005) and the cyclic lipopeptides surfactin and massetolide (Tran *et al*., 2007). Intriguingly, except for bacterial flagellin and for the yeast invertase glycopeptide, no other specific proteinaceous binding sites have been identified for MAMPs perception at the plant plasma membrane level. Surfactins are heptapeptides synthesized by *Bacillus* species (Fig. 1) via non-ribosomal peptide synthetases (NRPS) organized in iterative functional units called modules that catalyse the different reactions leading to peptide formation (Finking and Marahiel, 2004). Such biosynthetic systems lead to a remarkable heterogeneity among the lipopeptide products. They vary in the type and sequence of amino acid residues, the nature of the peptide cyclization and in the nature, length and branching of the fatty acid chain (Raaijmakers *et al*., 2006). The surfactin family also contains several variants with the same peptide length but different residues at specific positions. Usually, for each variant, *Bacillus* strains may co-produce several homologues of different length and isomery of the fatty acid chain (Ongena and Jacques, 2008).

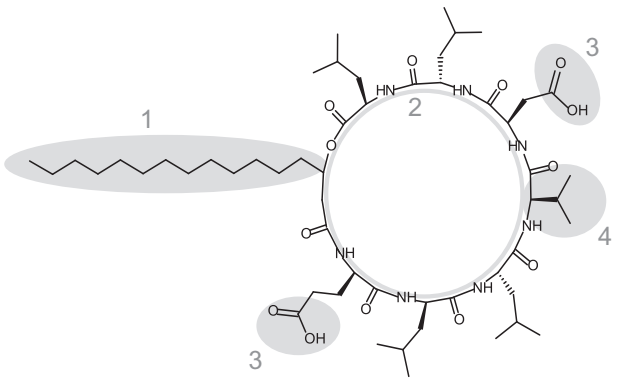

Fig. 1. Typical structure of surfactin A used in this study. Structural traits of the molecule that have been identified as being important for eliciting activity in this work (see Fig. 4) are highlighted in grey. (1) Surfactin homologues with less than 14 carbons in the fatty acid chain do not induce oxidative burst response as well as derivatives with opened peptide cycle (2) and/or alkylated acidic amino acids (3). Peptide-modified surfactin variants (4) also showed altered activity potential.

Previous work in our laboratory has demonstrated that surfactin is the main elicitor secreted by specific *Bacillus* strains displaying consistent ISR activity (Ongena *et al*., 2007; Ongena and Jacques, 2008). Surfactin also appeared to be the sole ingredient from *Bacillus amyloliquefaciens* S499 capable to stimulate a whole set of defence-related early responses in tobacco suspension cells (Jourdan *et al*., 2009). In addition to their interest for plant immunization, these lipopeptides also display versatile functions in the ecology of the producing strains and notably in biofilm formation, motility and in interactions with coexisting organisms, including bacteria, fungi, oomycetes or protozoan predators (Raaijmakers *et al*., 2010).

In contrast to the numerous investigations conducted on PTI-inducing MAMPs, little information is available about molecular mechanisms governing the recognition of ISR-specific elicitors by plant cells (van Loon *et al*., 2008; Varnier *et al*., 2009). In order to know if surfactin perception by plant cells is mediated by specific proteic receptors or not, two approaches were used in this work. We first tested multiple structural variants for their potential to induce oxidative burst in suspension-cultured cells and on tobacco roots. This working model allows the study of defence activation processes with good consistency and temporal resolution. Beside structure/activity relationship, a biophysical characterization of the interaction of surfactin with large unilamellar vesicles (LUVs) of different compositions by using isothermal titration calorimetry (ITC) was also performed with the aim to identify preferential membrane lipids or domains for interaction.

Results

Surfactin-triggered oxidative burst as marker of the induced defensive state

Oxidative burst typically occurs within minutes in response to MAMPs and the generated reactive oxygen species can act both directly as toxic substances against the pathogen and indirectly by reinforcing cell wall or by playing a signalling role to induce defence gene expression (Torres, 2010; Zipfel and Robatzek, 2010). Here we wanted to demonstrate that oxidative burst may serve as an appropriate marker of the defensive state for further investigations.

To that end, stimulation of extracellular hydrogen peroxide production by tobacco cells was measured using the luminol-based chemiluminescence assay and upon treatment with purified surfactins [as a mixture of homologues varying in the length of the acyl chain in the proportions 5/14/43/38 (%) for $C_{12}/C_{13}/C_{14}/C_{15}$ isoforms respectively]

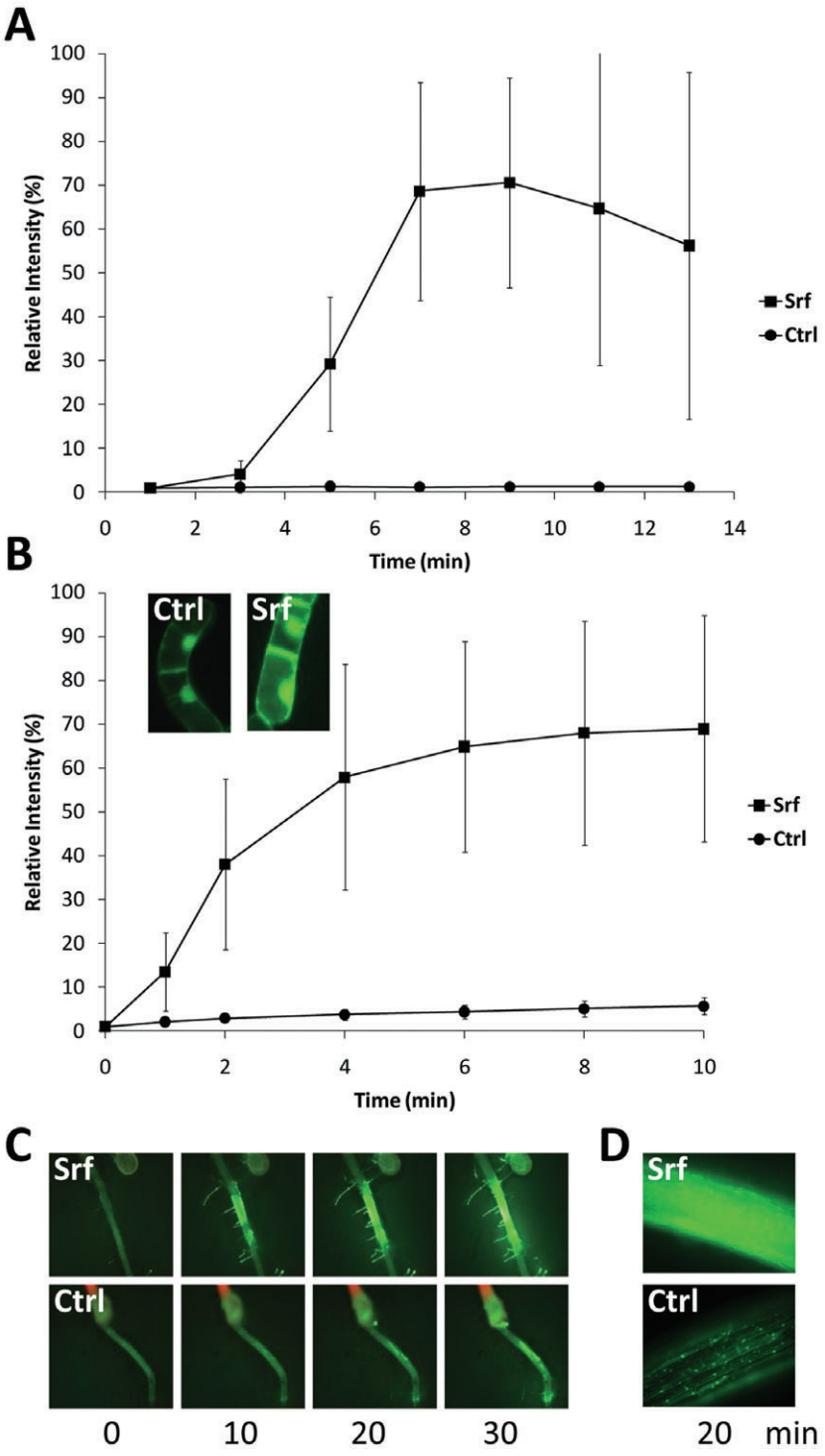

Fig. 2. Surfactin-induced reactive oxygen species (ROS) production.
A. Extracellular production of hydrogen peroxide by tobacco cells treated by 10 μM surfactin mix.
B. Intracellular accumulation of ROS in tobacco suspension cells upon the same treatment.
C. Kinetic of the intracellular accumulation of ROS in tobacco roots induced by 10 μM surfactin mix.
D. Intracellular accumulation of ROS in tomato roots induced by surfactin.
Extracellular H_2O_2 concentration was measured by chemiluminescence while intracellular ROS accumulation was detected by DCFH-DA staining. Control (Ctrl) consists in a treatment with a similar volume of methanol. All images were acquired with the same exposition time and light sensitivity. A slight increase in fluorescence is observed in all cases due to light-induced auto-oxidation of the dye. Vertical bars represent standard deviation of three and seven independent experiments for intracellular and extracellular production of hydrogen peroxide respectively.

synthesized by *B. amyloliquefaciens* strain S499. This surfactin mix extract clearly stimulated a transient oxidative burst within 4–5 min (Fig. 2A). No later refractory burst (Fig. 3) or cell death could be observed (Supplementary information 1). As shown in Fig. 2B, oxydative burst also occurs in the cytoplasm of the cultured cells with similar amplitude but more rapidly since fluorescence increase due to the oxidative stress-sensitive dye DCFH-DA was already visible after 1–2 min post treatment. Surfactin-induced ROS accumulation was also observed in root tissues of tobacco and tomato plantlets as determined with the same fluorimetric method (Fig. 2C and D).

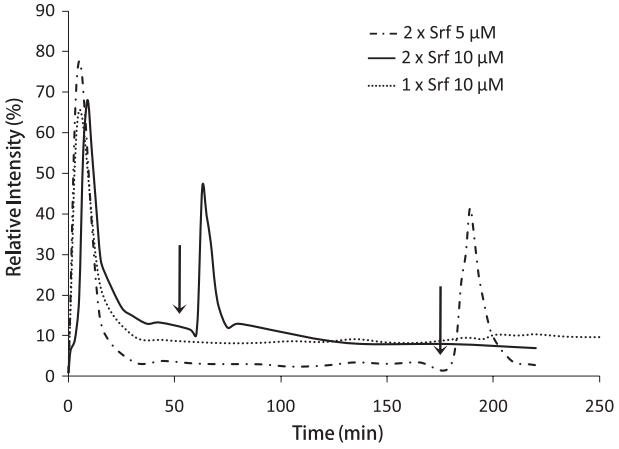

Fig. 3. No refractory state induced by repeated stimulation with surfactin. Extracellular release of hydrogen peroxide induced by two successive treatments of tobacco cells with surfactin mix. For two different concentrations and timings, re-addition of surfactin leads to a consistent albeit slightly lower response while no secondary burst has been observed upon single addition of surfactin.

The presence of high-affinity protein receptors for PAMPs in the plasma membrane is typically associated with the occurrence of some refractory state where host cells are no longer able to react to a second stimulation by the same compound because of irreversible saturation of the binding sites (Felix *et al.*, 1993; Freudenberg *et al.*, 1998). As illustrated in Fig. 3 for two different concentrations and timings, such a refractory state is not observed in the interaction with surfactin as a second treatment resulted invariably in a consistent oxidative burst response.

We then wanted to relate the observed oxidative burst triggering effect on tobacco suspension cells to induction of systemic resistance in whole plants. To that end, typical ISR experiments were conducted in which surfactin mix extract (10 µM) was applied to the roots of tobacco plantlets before infecting leaves with the pathogen *Botrytis cinerea* in order to avoid any direct contact and thereby any possibility of antagonistic activity. Under our experimental conditions, infection rates in disease control plants were comprised between 40% and 65%. In three independent bioassays, treatment with the lipopeptide led to 26%, 53% and 46% reduction of disease incidence compared with untreated but infected controls. Results of disease reduction in the last two assays are statistically significant with *P*-values of 0.014 and 0.012 respectively according to *t*-test for independent samples using Statistica software, Stat Soft.

The eliciting activity of surfactin relies on specific structural traits

As ROS accumulation represents a sensitive and appropriate marker for defence activation by surfactin in host plant cells, we further used this phenomenon to study the structure/activity relationship. All structural derivatives that were generated and used for that study are represented in Fig. 4A. First, we tested the importance of the length of the fatty acid chain for the eliciting potential of the molecule. To that end, the various homologues present in the pre-purified surfactin mix extract used above were isolated by semi-preparative HPLC and tested independently for oxidative burst induction. Our data revealed that homologues with the shortest lipid chains (C12 and C13) failed to induce any hydrogen peroxide release (Fig. 4B). In contrast, C14 and C15 surfactins triggered a significant response that probably accounts for most of the activity of the surfactin mix sample. The active C14 homologue was further chemically modified via alkylation and/or saponification in order to appreciate the importance of cyclization and presence of charges (two acidic residues) in the peptide. It appears that all the linear, methylated and linear/methylated derivatives have lost eliciting activity on tobacco cells (Fig. 4B).

For some bacteria, the NRPS machinery allows precursor-directed modulation of the amino acid content of the peptide produced by a given strain because of reduced specificity of adenylation domains regarding the nature of the amino acid residue it can activate (Grangemard *et al.*, 1997; Kowall *et al.*, 1998). We wanted to take advantage of such flexibility to generate surfactin variants after growing the strain in a medium supplemented with L-Leu, L-Val or L-Ileu as sole amino acid source. Feeding with these residues led to additional peaks in the surfactin signature determined by LC-ESI-MS analysis of supernatant extracts. Amino acid analysis of hydrolysates and in-source fragmentation in the mass spectrometer confirmed the nature of the substitutions at positions 4 and 7 (Supplementary information 2). In all cases, activities of these peptidic variants were reduced compared with the one of unmodified surfactin homologues with similar fatty acid chain length (Fig. 4C). A substitution of L-Val by L-Leu in position 4 of the C14 and C15 homologues affected more markedly the activity of the C15 than the one of the C14 suggesting that efficacy of the compound relies on a combined effect of acyl chain length and the residue position in the peptide. In contrast, a substitution of Leu residue by a less hydrophobic amino acid was less detrimental for the activity than a substitution by a more hydrophobic residue since both C15 Leu4 and C15 Ile showed a three times lower activity than C15 Val7 which itself lost 50% of the natural C15 homologue activity.

We also evaluated the competition between active and inactive surfactin variants for potential recognition sites on cultured cells. Figure 5 shows that subsequent addition of C15 homologue after a first treatment with inactive C13

A

	Origin	Structure
C12	Natural prod.	$CH_3-(CH_2)_8-CH-CH_2-CO\rightarrow Glu\rightarrow Leu\rightarrow Leu\rightarrow Val\rightarrow Asp\rightarrow Leu\rightarrow Leu-O$
C13	Natural	$CH_3-(CH_2)_9-CH-CH_2-CO\rightarrow Glu\rightarrow Leu\rightarrow Leu\rightarrow Val\rightarrow Asp\rightarrow Leu\rightarrow Leu-O$
C14	Natural	$CH_3-(CH_2)_{10}-CH-CH_2-CO\rightarrow Glu\rightarrow Leu\rightarrow Leu\rightarrow Val\rightarrow Asp\rightarrow Leu\rightarrow Leu-O$
C15	Natural	$CH_3-(CH_2)_{11}-CH-CH_2-CO\rightarrow Glu\rightarrow Leu\rightarrow Leu\rightarrow Val\rightarrow Asp\rightarrow Leu\rightarrow Leu-O$
C14 m	Chemical	$CH_3-(CH_2)_8-CH-CH_2-CO\rightarrow GluCH_3\rightarrow Leu\rightarrow Leu\rightarrow Val\rightarrow AspCH_3\rightarrow Leu\rightarrow Leu-O$
C14 l	Chemical	$CH_3-(CH_2)_8-CH-CH_2-CO\rightarrow GluCH_3\rightarrow Leu\rightarrow Leu\rightarrow Val\rightarrow AspCH_3\rightarrow Leu\rightarrow Leu-O$
C14 lm	Chemical	$CH_3-(CH_2)_{10}-CH-CH_2-CO\rightarrow Glu\rightarrow Leu\rightarrow Leu\rightarrow Val\rightarrow Asp\rightarrow Leu\rightarrow Leu-O$
C14 Leu4	Precursor-directed	$CH_3-(CH_2)_{10}-CH-CH_2-CO\rightarrow Glu\rightarrow Leu\rightarrow Leu\rightarrow Leu\rightarrow Asp\rightarrow Leu\rightarrow Leu-O$
C14 Ile	Precursor-directed	$CH_3-(CH_2)_{10}-CH-CH_2-CO\rightarrow Glu\rightarrow Leu/Ile\rightarrow Leu/Ile\rightarrow Leu/Ile\rightarrow Val\rightarrow Asp\rightarrow Leu/Ile\rightarrow Leu/Ile-O$
C15 Val7	Precursor-directed	$CH_3-(CH_2)_{11}-CH-CH_2-CO\rightarrow Glu\rightarrow Leu\rightarrow Leu\rightarrow Val\rightarrow Asp\rightarrow Leu\rightarrow Val-O$
C15 Leu4	Precursor-directed	$CH_3-(CH_2)_{11}-CH-CH_2-CO\rightarrow Glu\rightarrow Leu\rightarrow Leu\rightarrow Leu\rightarrow Asp\rightarrow Leu\rightarrow Leu-O$
C15 Ile	Precursor-directed	$CH_3-(CH_2)_{11}-CH-CH_2-CO\rightarrow Glu\rightarrow Leu/Ile\rightarrow Leu/Ile\rightarrow Leu/Ile\rightarrow Val\rightarrow Asp\rightarrow Leu/Ile\rightarrow Leu/Ile-O$

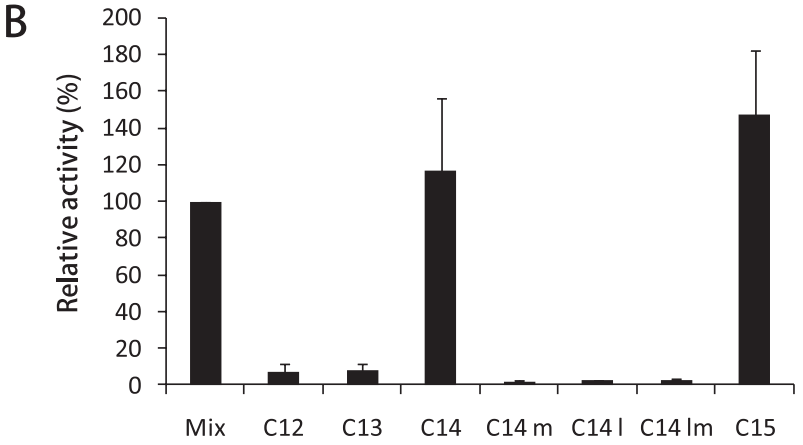

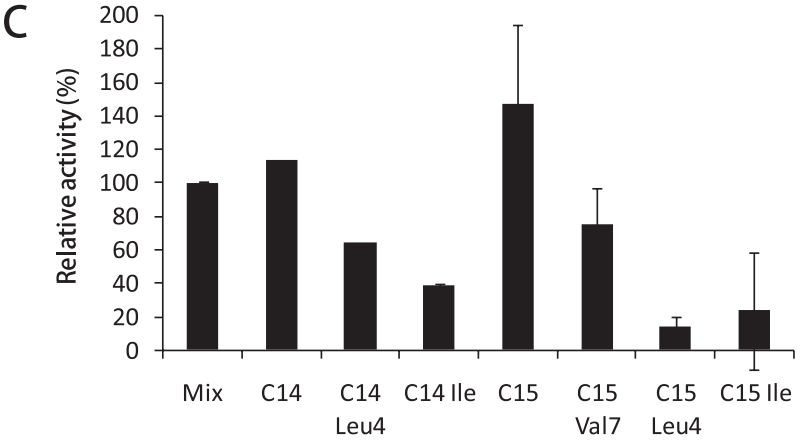

Fig. 4. Structure–activity relationship of surfactin. Surfactin variants used in this study are described in (A). For C14 Ileu and C15 Ileu, the exact position of the Ileu residue within peptide cycle was not determined (see *Supporting information*). Hydrogen peroxide release by tobacco cells upon treatment with 15 μM surfactin variants is described in (B) for compounds with variable lipid chain from 12 (C12) to 15 carbons (C15) and for methylated and linear derivative of the C14 homologue and in (C) for compounds varying in the peptide sequence. The 15 μM concentration led to the highest responses with active surfactin homologues and was therefore selected in order to increase the difference of activity between active and less or non-active isoforms. Data are expressed as relative activity compared with the one of surfactin mix containing naturally produced homologues. Data are means and standard deviations calculated from three independent experiments.

leads to a full production of ROS. This was also observed following a first addition of C14 that has been completely inactivated by methylation or, to a slightly lower extent, upon cell pre-treatment with C15 Leu/Ile substitution. Results obtained in assays performed with other inactivated forms (C12, cyclized C14 surfactins, data not shown) are not represented for clarity but were similar.

High affinity of long-chain surfactin homologues for cell membranes

Upon addition to tobacco cell suspension at a concentration similar to the one inducing oxidative burst, the long-chain homologues C14 and C15 almost completely disappear from the medium within 10 min and are mainly

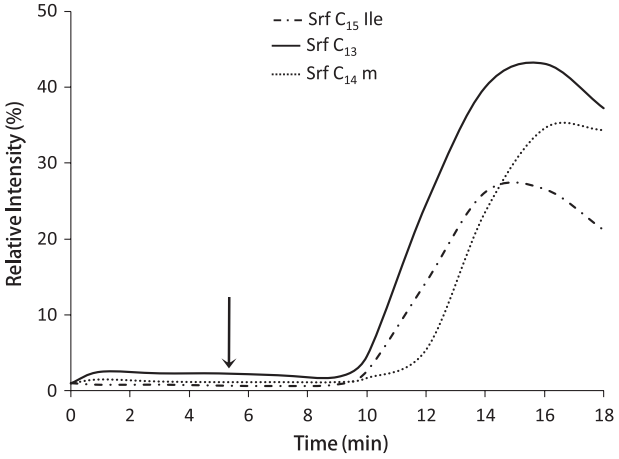

Fig. 5. Competition experiments between surfactin isoforms. Extracellular release of hydrogen peroxide induced by 10 μM surfactin C15 homologue when applied 10 min after a first stimulation at the time indicated by the arrow with non- or less active C13/C14m/C15Ile isoforms. Data are from one representative experiment and similar results were obtained in two other repeats.

recovered from membranes after fractionation of the treated cells (Fig. 6A and B). In contrast, the binding kinetic of inactive isoforms on tobacco cells is significantly slower and they remain mostly in the supernatant fraction (data not shown) suggesting a much lower affinity for the plant cell membrane. So the differential ROS-inducing activity among the various homologues and derivatives of surfactin is also reflected by differences in their level of interaction with tobacco cells. In all cases, lipopeptide quantities recovered from the intracellular pool are very low indicating that these compounds do not readily penetrate through the tobacco cell wall. Similar kinetic and partitioning trends were obtained by using intact roots of tobacco plantlets instead of cell suspension cultures. The surfactin-induced oxidative burst is transient but binding of the lipopeptide to the cell membrane is long-lasting as extraction performed 5 days later (on both cells and roots) allowed to recover most of the initial quantities. In all instances, the initial amount of surfactin added to cells or roots was fully recovered at the end of the experiment by summing supernatant, intracellular and membrane pools. Moreover, surfactin was extracted from membranes in its intact form as revealed by HPLC-MS. It suggests that transiency of the oxidative burst response does not result from lipopeptide degradation at the membrane level. There is also no significant change in insertion rate of the C14 homologue after pre-treatment of cells with proteases (trypsin and pronase) in order to inactivate putative plasma membrane-associated proteic binding site (data not shown).

In order to get further insights into the nature of the interaction between surfactin and plant cell membranes, ITC experiments were performed using LUVs (Berglund *et al.*, 2004) and binding isotherms of lipopeptide–lipid interactions were determined by calorimetric measurements upon titration of lipid dispersions into peptide solutions. We first compared binding of surfactin to palmitoyl oleoyl phosphatidyl choline (POPC) and palmitoyl linoleoyl phosphatidyl choline (PLPC), the predominant phospholipids of mammalian and plant membranes respectively. Parameters obtained from the fitting of cumulative reaction heats as a function of lipid concentration demonstrate that surfactin interacts spontaneously ($\Delta G_D^{w\to b} < 0$) with both types of vesicles in an endothermic ($\Delta H_D^{w\to b} > 0$) and entropy-driven ($\Delta S_D^{w\to b} > 0$) process (Fig. 7A and Supplementary information 3). Based on the affinity constant (K) (Fig. 7A), the binding of surfactin to POPC is only slightly lower than to PLPC (see supplementary information 3 for detailed data).

Isothermal titration calorimetry-based thermodynamic studies conducted on lipid vesicles mimicking the plasma membrane of root cells (phosphatidyl choline/phosphatidyl ethanolamine/stigmasterol/sitosterol/glucosylceramide; 40/34/8/5/13 in %) also confirmed a clearly different behaviour between long bioactive and shorter inactive surfactin homologues (Fig. 7B). Membrane partitioning for both C13 and C14 forms tested individually is basically endothermic and entropy-driven, as observed by using the surfactin mix sample. However, based on *K*-values, the affinity of the C14 homologue for root cell membrane model is four times higher than the one calculated for C13.

Preferential interaction of surfactin with specific lipid organization

The most important phase transition in lipids bilayers under equilibrium conditions in the context of lipid domains formation is the so-called main transition (Simons and Vaz, 2004), which corresponds to the change of the membrane from a solid phase with conformationally ordered lipid acyl chains (solid ordered, So) to a liquid phase with conformationally disordered lipid acyl chains (liquid disordered, Ld). In presence of sterols, a third liquid-ordered phase (Lo) has been shown. All these phases may also coexist in some ternary lipid mixtures.

Interestingly, a much higher binding affinity (based on *K*-values) of surfactin on LUVs was observed by using a mixture of PLPC with a high-melting-temperature lipid, dipalmitoyl phosphatidyl choline (DPPC) (Fig. 7A, Supplementary information 3), which are thought to form coexisting Ld and So phases. Some lipopeptides other than surfactin strongly interact with sterols, forming destabilizing complexes within the cytoplasmic membrane of target cells (Maget-dana and Peypoux, 1994). The influence of sterols was thus tested by adding stigmasterol (the main representative of plant membrane sterols) in appropriate

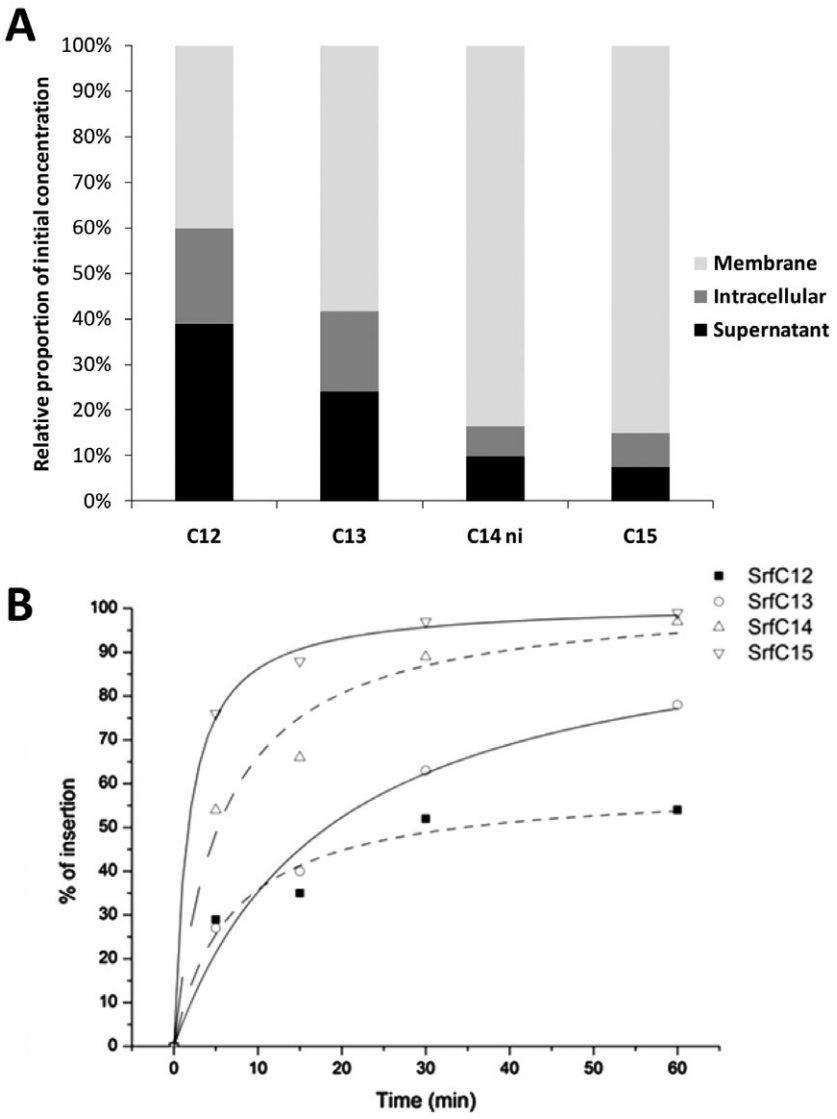

Fig. 6. Binding profile of surfactin isoforms on tobacco cells.
A. Relative abundance (% of the initial concentration) of the various surfactin homologues in supernatant, intracellular and cell membrane fractions recovered 3 h after their addition (5 μM in supernatant) to a tobacco cell suspension.
B. Kinetics of insertion of various surfactin homologues within tobacco cells based on decrease of the concentration (initial 5 μM) measured in the supernatant. In both cases, data presented are means calculated from two independent assays that yielded similar results.

proportions within LUV lipids but no significant effect on surfactin binding was observed (Fig. 7A).

In order to investigate the mode of interaction of surfactin with different patterns of lipid domains, we used a ternary system POPC/sphingomyelin/cholesterol to generate different phases: liquid ordered (Lo), liquid disordered, solid ordered (So) or the coexistence of phases (De Almeida *et al.*, 2003). Our results show that association of surfactin with the bilayers is favoured for LUVs containing So domains (Fig. 7C). Affinity for other coexisting domains (Lo+So < Ld+So < Ld+Lo+So < So) decreases even if binding is still entropy-driven and endothermic. Binding to 'raft like' domains (Lo+Ld) is low in comparison with domains containing So phase. Meanwhile, as the affinity is three times higher for Ld phase than Lo phase, this suggests that the affinity for the Ld+Lo phases is governed by the affinity for the Ld part.

Discussion

The cyclic lipopeptide surfactin is efficient at triggering systemic resistance in various plants but, as for most of the other ISR elicitors from non-pathogenic rhizobacteria and in contrast to pathogen MAMPs with associated receptors (Bittel and Robatzek, 2007), almost nothing is known about their recognition process at the plant cell surface. To that end, we used oxidative burst as marker of the defensive state. Upon treatment with surfactins, ROS accumulation occurs not only extracellularly but also even more rapidly in the cytoplasm of induced cells. This suggests that, as the plasma membrane-associated NADPH oxidase is required for consistent burst induced by the lipopeptide (Jourdan *et al.*, 2009), ROS formation may either be quenched by the cell wall and by extracellular peroxydases or originate from internal compartments. The

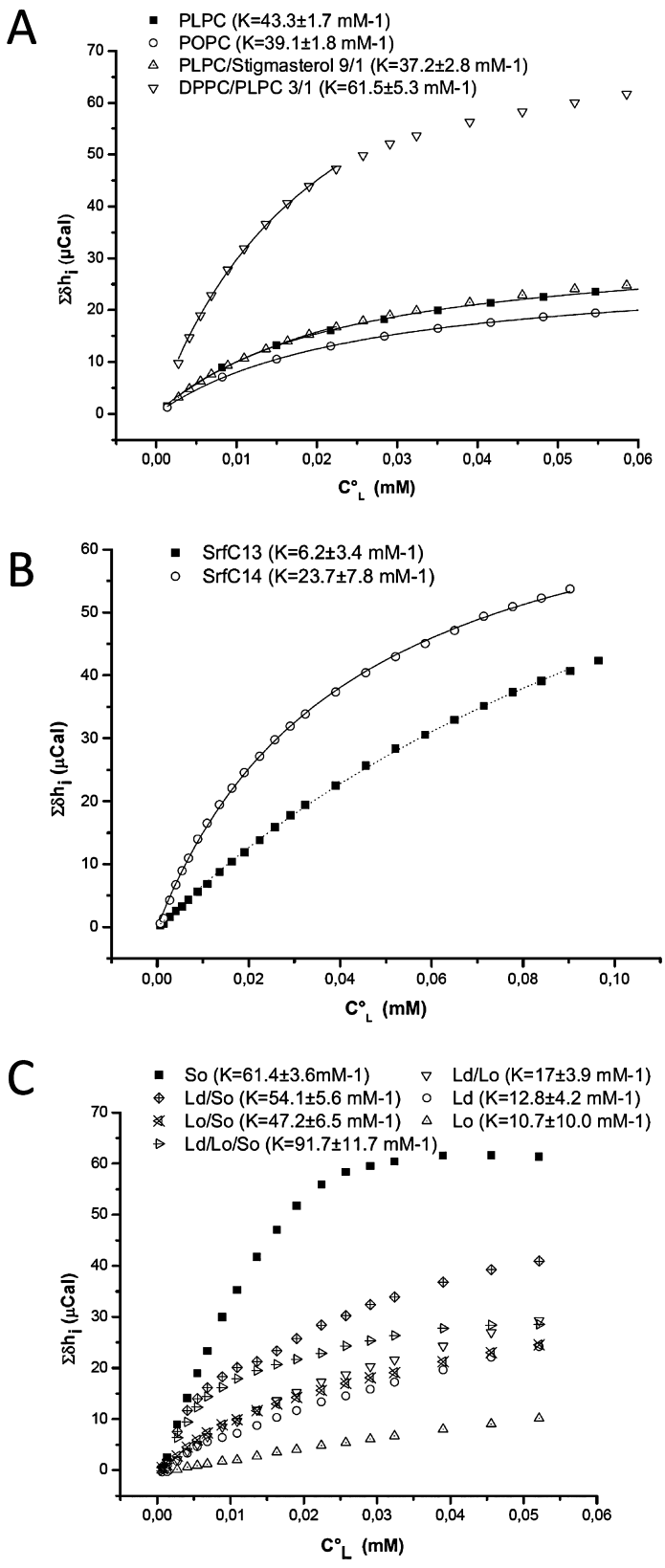

Fig. 7. Cumulative reaction heats as a function of lipid concentration.
A. Titration of 10 µM surfactin mix with 1 mM vesicles of different composition, derived from ITC measurements at 25°C.
B. Titration of 10 µM surfactin C13 and C14 homologues with 1 mM vesicles mimicking plant root plasma membrane composition from ITC measurements at 23°C.
C. Titration of 10 µM surfactin mix with 1 mM vesicles with various lipid phases composition from ITC measurements at 23°C.
So, solid ordered phase; Lo, liquid ordered phase; Ld, liquid disordered phase. The solid line corresponds to mean theoretical fits from three independent experiments and thermodynamic parameters of membrane binding are calculated according to the cumulative heat model (Heerklotz and Seelig, 2001).

latter hypothesis suggest that extracellular ROS production may better function as an amplifying loop of preceding internal pool as already demonstrated upon perception of the fungal PAMP cryptogein (Kunze *et al*., 2004). Opposed to the early, transient but non-specific burst induced following perception of PAMPs, the effector-triggered HR is typically related to the late (within hours) occurrence of a secondary consistent ROS accumulation which is coupled with the HR. It usually occurs in ETI upon successful pathogen recognition (Boller and Felix, 2009; Torres, 2010) but some PAMPs such as flagellin also seem to be able to induce HR (Naito *et al*., 2008). Such a secondary burst and cell death are not observed in surfactin-elicited tobacco cells. This suggests that the lipopeptide is perceived as a classical MAMP at the cell surface rather than as an effector delivered inside the target cells and detected by cytoplasmic proteins with a nuclear binding site.

In a first approach involving structure/activity relationship, we observed a significantly decreased defence-inducing activity for metabolically engineered derivatives with Val/Leu, Leu/Val, Leu/Ile or Val/Ile substitutions in the peptide. Such very limited structural changes may alter the hydrophobicity of the peptide part but are not expected to drastically modify the conformation of some epitope that could be perceived by putative protein receptors. Our results also showed the absence of competition between surfactin homologues with identical peptide cycle again suggesting that their recognition does not rely on very specific structural traits in that part of the molecule. Moreover, in contrast with PAMPs perceived at nanomolar concentrations by their receptors, lipopeptides are active in the micromolar range (Tran *et al*., 2007; Jourdan *et al*., 2009). We also showed here that surfactin affinity is apparently fully conserved on protease pre-treated cells and that a first contact of tobacco cells with surfactin does not preclude subsequent reactivity to a second application meaning that possible saturation of highly effective fixation sites is not involved. The existence of specific receptors for bacterial lipopeptides in tobacco cells is thus questionable.

Surfactin typically displays a 'horse saddle' topology harbouring a minor polar and a major hydrophobic domain in the peptide chain. For an isolated molecule in polar solvent, the aliphatic tail of the fatty acid is probably in a folded configuration along the hydrophobic domain of the peptide, stabilized by interactions with leucine and valine side-chains (Peypoux *et al*., 1999; Bonmatin *et al*., 2003; Shen *et al*., 2009). It is thus obvious that both the nature and place of the various amino acid residues in the cyclized peptide moiety strongly contribute to the stability of this conformation. The significant loss of functionality of the peptide variants of surfactin used in this study might therefore be explained by a more subtle destabilizing effect regarding the tridimensional structure of the molecule. Such an impact of individual substitutions on the spatial positioning of the acyl chain relative to the peptide backbone is obvious in the case of surfactin and other closely related lipopeptides (Bonmatin *et al*., 2003; Volpon *et al*., 2007). A substitution of Val in position 4 by Leu or Ile is known to significantly improve surface properties (Grangemard *et al*., 1997; Bonmatin *et al*., 2003). It reinforces surfactant behaviour and probably causes changes in the organization of surfactin molecules at the air–water interface, and thus possibly at the membrane level (Bonmatin *et al*., 1995). It is worth noting that even if multiple studies have characterized structures and surface properties of new surfactins, very few have focused on biological activities of such variants. By purifying for the first time a sufficient amount of metabolically engineered surfactin variants, we demonstrate that a theoretical increase of physical properties (surface tension decrease, critical micelle concentration) for variants with Leu in position 4 does not necessarily correlate with an increased activity on living organisms, at least on plant cells.

Alkylation of acidic amino acids and breakdown of the peptide cycle ring completely suppressed the burst-inducing activity of surfactin on tobacco cells. These results illustrate the importance of a specific hydrophilic/lipophilic balance and spatial conformation for perception of the lipopeptide at target sites on plant cell membranes. Both membrane activity and lytic potential on erythrocytes were also shown to increase with the number of ionic charges (Morikawa *et al*., 2000; Francius *et al*., 2008) and the cyclic structure (Dufour *et al*., 2005). Cyclization thus benefits not only stability and rigidity of the compound, but also its biological activity. It is clear now that negative charges and cyclic structure also benefit perception by plant cells. A complete loss of activity was observed for surfactins with fatty acid chains shorter than 14 carbons and a higher activity was observed for the predominant C15 homologue. Such an important role for the aliphatic tail has already been documented for other biological activities of lipopeptides and is explained by the fact that it readily inserts into phospholipid bilayers (Bonmatin *et al*., 2003; Carrillo *et al*., 2003; Eeman *et al*., 2006; Heerklotz and Seelig, 2007). Despite the ball-like 3D conformation of surfactin in solution, some specific dynamic changes may occur in the fatty acid position relative to the peptide moiety to favour its insertion in lipid layers (Deleu *et al*., 2003; Tsan *et al*., 2007).

Surfactin clearly acts by disrupting bacterial, viral and erythrocyte cell membranes (Vollenbroich *et al*., 1997; Kracht *et al*., 1999; Huang *et al*., 2006). In contrast, the molecule is poorly fungitoxic and does not display any marked toxicity on plant (Supplementary information 1 and Jourdan *et al*., 2009) and mammalian cell lines (Kim

et al., 2007) at similar concentrations. The outcome of the interaction between surfactin and target cells thus appears quite specifically dictated by the lipid content and/or structure of the plasma membrane. Our ITC results confirm that the lipopeptide has a high affinity for membrane lipids driven by hydrophobic interactions. However, this interaction is not favoured in the presence of lipids typical from plant cells and addition of stigmasterol in binary mixtures with PLPC did not affect the level of binding (Fig. 7). Thus surfactin does not have a specific affinity for plant sterols in contrast to other *Bacillus* lipopeptides such as iturin (Maget-dana and Peypoux, 1994) and fengycin (Eeman *et al*., 2009). This may thus partly explain the differential bioactivities of these structurally close-related lipopeptide families on various cell types. However, a higher sterol proportion in lipid ternary mixtures leading to the formation of Lo domains significantly decreased binding of surfactin. Sterols are intercalated between fatty acyl chains of phospholipids molecules and extend their side-chain deeply into the interior of the bilayers. This could explain that they restrict the access of lipopeptides to the inner side of membranes. The presence of cholesterol in the phospholipid layer is known to attenuate the destabilizing effect of surfactins (Carrillo *et al*., 2003) as evidenced for a number of other membrane-destabilizing compounds (Pott *et al*., 1996; Maula *et al*., 2009).

On the other hand, the presence of sterols in higher proportions in ternary lipid mixtures can more globally influence the structure and conformation of the bilayer through the formation of Lo domains. Such changes strongly and negatively impact on surfactin binding as shown in Fig. 7C. More generally, our results highlight the close relationship between the physical structure of the lipid bilayer and its association with surfactin. The lipopeptide clearly exhibits enhanced binding to So-containing vesicles. It is known that even if the membrane phase state is uniform, the lipid packing inside these domains is heterogeneous and displays an orientational texture (Bernchou *et al*., 2009). It gives a highly structured and condensed membrane with regular corrugations in its topography called ripple phase. Even if at physiological temperatures, cellular membranes probably coexist mainly as fluid and liquid-ordered domains, it is likely that rippled solid ordered phases transiently form. The affinity of surfactin for So phases containing bilayers may be due to higher hydrophobic interactions in the interior of the bilayers compared with highly mobile and unsaturated lipid chains of the Ld phase lipids and the sterol congested Lo phases. The entropy-driven nature of the process may be explained by a gain of water disorder after dehydration and a lower freedom of movement of lipid chains but also by deformation and structural changes of the lipid bilayer (Jelokhani-Niaraki *et al*., 2008).

In summary, surfactin perception could thus rely on specific features of the plant plasma membrane regarding composition and/or organization of the lipid bilayer. Even if a low-affinity receptor-driven perception cannot not be completely ruled out so far, results of this work suggest that surfactin may insert and disturb lipid compartmentalization or induce curvature constraints in host cell membranes. As no significant cell death has been observed by using lipopeptide concentrations below 20 μM, such disturbance is not sufficient to provoke cell envelop disruption. However, it can lead to direct activation of mechanosensitive channels or proteins involved in signalling which in turn activate a biochemical cascade of molecular events leading to the establishment of defensive responses. The components of biological membranes are laterally diversified into transient assemblies of varying content and order, and many proteins are suggested to be activated or inactivated by their localization in or out of plant membrane microdomains displaying different physical phases. Recently, signalling involved proteins have been shown to be differentially associated to plant membranes microdomains after cryptogein challenge (Stanislas *et al*., 2009), suggesting that the activity of membrane proteins may be more dependent on the surrounding lipid organization than previously estimated. In future work, we want to test the hypothesis of a surfactin-induced lipid reorganization that triggers some recruitment and activation of key defence-related enzymes (NADPH oxidase) in particular microdomains of the plasma membrane.

Experimental procedures

Preparation and analysis of surfactin variants

The mixture of surfactin (95% purity) was obtained from *B. amyloliquefaciens* strain S499 and the various homologues were purified from this mixture as described previously (Jourdan *et al*., 2009). In all instances, surfactin was used from a methanolic stock solution 1 mg ml^{-1}. Linear derivatives of the C14 surfactin homologue were synthesized in the Laboratory of Industrial Biology of the University of Liège/Gembloux Agro-Bio Tech (Belgium) using the method described by Dufour and associates (Dufour *et al*., 2005). Peptide-modified surfactins were generated by culturing strain S499 in a medium containing (i) a mixture of sugars (glucose 34%, fructose 57%, maltose 8%, ribose 0.75% in weight) at a final concentration of 5 g l^{-1}, (ii) a mixture of organic acids (citrate 77%, succinate 19%, malate 2%, fumarate 0.5%) at a final concentration of 4.5 g l^{-1}, and (iii) amino acids at 0.5 g l^{-1} with casamino acids used for control replaced by L-Leu, L-Val or L-Ileu. One hundred millilitres of the medium was sterilized in 500 ml flasks and amino acid solution was then added by filter sterilization. Strain S499 was incubated for 72 h at 37°C under agitation.

Linear, methylated and peptide-modified surfactins were purified by HPLC using the isochratic method described for naturally produced lipopeptides. The molar ratio of the amino acids was

determined by analysing acid hydrolysed products (HCl 6 N at 145°C for 4 h under vaccum). Amino acid analysis was performed according to the method developed by Agilent Technologies with online derivatization using o-phthalaldehyde and further resolution on a Zorbax Eclipse AAA column. All surfactin variants used in this study were finally checked for purity/structure and quantified by reversed phase HPLC coupled with mass spectrometry as described in Supplementary information 2. Assignment of fragmentation ions was supported by data from previous studies (Jenny *et al*., 1991; Kowall *et al*., 1998).

Reactive oxygen species accumulation in tobacco cells

Tobacco cells (*Nicotiana tabacum* L. cv. Bright Yellow-2) were cultivated and prepared for experiments as already described (Jourdan *et al*., 2009). Intracellular ROS accumulation was monitored with the oxidant-sensing fluorescent probe 2′,7′-dichlorodihydrofluorescein diacetate (DCFH-DA). Tobacco cells were loaded for 5 min with 25 μM DCFH-DA. Cells were then treated with 15 μM surfactin. One hundred microlitres of the suspension was analysed with a plate fluorometer (Wallac Victor 1420) (λexc 485 nm; λem = 535 nm; measurement time: 0.1 s). Tomato roots pictures were obtained by loading 10 μM DCFH-DA for 5 min on roots of 15-day-old tobacco plants grown on Petri dishes (MS salt medium five times diluted added to 14 g l^{-1} agar) and treated with 10 μM surfactin. Pictures were taken with a fluorescent Axioskop2-type microscope (505 nm excitation Filter, Carl Zeiss Jena GmbH, Germany). The production of extracellular ROS was monitored by a chemiluminescence measurement of H_2O_2 from the ferricyanide-catalysed oxidation of luminol using a luminometer (TD-20/20 Luminometer, Turner Designs, Fresno, CA, USA). After treatment with surfactin, a 50 μl aliquot of the cell suspension (final concentration 0.15 gFW ml^{-1}) was added to 100 μl of 50 mM phosphate buffer (pH 7.9) and 100 μl of 1.1 mM luminol in phosphate buffer. The reaction was started by addition of 100 μl of freshly prepared 14 mM $K_3[Fe(CN)_6]$ and the signal was integrated over the first 30 s after reaction start.

Biotests for induced systemic resistance

Induced systemic resistance assays were performed on tobacco plants grown hydroponically from sterilized seeds in a growth chamber under controlled conditions (26°C) for 5–6 weeks. Plant roots were treated with a methanolic solution of 10 μM surfactin or with the same volume of pure methanol for controls and transferred to a high humidity chamber (19 ± 2°C) for 24 h before leaf infection with *B. cinerea*. This was achieved by inoculating the fourth leaf with eight drops of spore suspension following the same method as described (Ongena *et al*., 2005). Experiments contained at least 10 plants per treatment and disease incidence was expressed in terms of the percentage of *B. cinerea* lesions that clearly grew out of the inoculum drop zone to produce spreading lesions 4–5 days post infection.

Kinetics of insertion and distribution of lipopeptides within tobacco cells

At various times following addition of surfactin to tobacco cell suspensions at 0.01 gFW ml^{-1}, 150 μl of the suspension was collected and centrifuged for 5 min at 5000 r.p.m. One hundred microlitres of the supernatant was diluted in the same volume of MeOH and then subjected to HPLC-MS for quantification. At the end of the experiment, remaining suspension was centrifuged. Supernatant was analysed as before while the cell pellet was resuspended in HEPES medium (same volume as discarded supernatant to keep 0.01 g cells ml^{-1}) and frozen. Thawed solution was then subjected to ultrasonic bath for 10 min and centrifuged. Supernatant was analysed as before while cell pellet was resuspended in MeOH (same volume as discarded supernatant to keep 0.01 g cells ml^{-1}). After vortexing and sonication, this solution was centrifuged and 100 μl of the supernatant was diluted in the same volume of HEPES medium before HPLC-MS quantification.

Vesicle preparation

POPC, PLPC, DPPC, soybean PC, soybean PE, glucosylceramide, stigmasterol and palmitoyl sphingomyelin (PSM) were purchased from Avanti Polar Lipids (Birmingham, AL). Synthetic β-sitosterol was from Sigma-Aldrich (purity > 95%). All other chemicals were from Sigma-Aldrich. These lipid substances were used without further purification. All measurements were made in buffer (150 mM NaCl, 10 mM TRIS, 1 mM EDTA; pH 8.5). Lipid mixtures were dried from a chloroform/methanol (2/1; v/v) solution under reduced pressure in a rotavapory evaporator at 30°C and then kept under vacuum overnight. The lipid film was hydrated in buffer during 1 h at 45°C with vortex mixing applied every 15 min and then subjected to five freeze/thaw cycles. The solution was sonicated six times 2 min at 2 min interval under 117 watts power using a sonicator tip with 3 mm diameter (Vibracell 75185). Our plant root plasma membrane model was based on the work of Berglund *et al*. (2004). We used LUV with lipid composition in mol%: Soy-Phosphatidylcholine: 40; Soy-Phosphatidylethanolamine: 34; Glucosylceramide: 13; Stigmasterol: 8; β-Sitosterol: 5. LUV mimicking plant root plasma membrane and LUV of different lipid phase composition were prepared by extrusion through two stacked Nuclepore polycarbonate membranes of 100 nm pore size. During the experiments, vesicles were stored above their melting temperature to avoid fusion events.

ITC assays

Isothermal titration calorimetry was performed with a VP-ITC Microcalorimeter (Microcal, Northampton, USA). The calorimeter cell (Volume of 1.4565 ml) was filled with a 10 μM lipopeptide solution in buffer. The syringe was filled with a suspension of LUV at a lipid concentration of 1 mM and a series of injections was performed (Vinj.: 1–15 μl) at constant time intervals (6 min) at 25°C for vesicles obtained by sonication and 23°C for LUV obtained by extrusion. The solution in the titration cell was stirred at 305 r.p.m. Prior to each analysis, all solutions were degassed using a sonicator bath. The heats of dilution of vesicles were determined by injecting vesicles in buffer and subtracted from the heats determined in the experiments. Data were processed by software Origin 7 (Originlab, Northampton, USA). For lipid size measurements, the average size of SUV suspension was determined at 23°C by dynamic light scattering (DLS) using a Zetasizer nano ZS (Malvern instruments, UK). The ITC data were

evaluated by using the model detailed in Supplementary information 3 and described by Heerklotz and Seelig (2001).

Acknowledgements

This work received financial support from the National Funds for Scientific Research (F.R.S.-F.N.R.S.) and from the EU-Interreg (programmes F.R.F.C. n° 2.4.628.10F, Crédit aux Chercheurs n° 1.5.192.08F and PHYTOBIO Project) (Belgium). G. Henry is recipient of a grant from the F.R.I.A. (Formation à la Recherche dans l'Industrie et l'Agriculture). M. Deleu and M. Ongena are research associates and E. Jourdan is post-doctoral researcher at the F.R.S.-F.N.R.S. The authors thank Harry Razafindralambo for the measurement of lipid vesicle size.

References

Bakker, P.A.H., Pieterse, C.M.J., and Van Loon, L.C. (2007) Induced systemic resistance by fluorescent *Pseudomonas* spp. *Phytopathology* **97:** 239–243.

Berglund, A.H., Larsson, K.E., and Liljenberg, C.S. (2004) Permeability behaviour of lipid vesicles prepared from plant plasma membranes – impact of compositional changes. *Biochim Biophys Acta Biomembr* **1682:** 11–17.

Bernchou, U., Brewer, J., Midtiby, H.S., Ipsen, J.H., Bagatolli, L.A., and Simonsen, A.C. (2009) Texture of lipid bilayer domains. *J Am Chem Soc* **131:** 14130–14131.

Bittel, P., and Robatzek, S. (2007) Microbe-associated molecular patterns (MAMPs) probe plant immunity. *Curr Opin Plant Biol* **10:** 335–341.

Boller, T., and Felix, G. (2009) A renaissance of elicitors: perception of microbe-associated molecular patterns and danger signals by pattern-recognition receptors. *Annu Rev Plant Biol* **60:** 379–406.

Bonmatin, J.M., Labbe, H., Grangemard, I., Peypoux, F., Magetdana, R., Ptak, M., and Michel, G. (1995) Production, isolation and characterization of [Leu(4)]surfactins and [Ile(4)]surfactins from *Bacillus subtilis*. *Lett Pept Sci* **2:** 41–47.

Bonmatin, J.M., Laprevote, O., and Peypoux, F. (2003) Diversity among microbial cyclic lipopeptides: iturins and surfactins. Activity–structure relationships to design new bioactive agents. *Comb Chem High Throughput Screen* **6:** 541–556.

Carrillo, C., Teruel, J.A., Aranda, F.J., and Ortiz, A. (2003) Molecular mechanism of membrane permeabilization by the peptide antibiotic surfactin. *Biochim Biophys Acta Biomembr* **1611:** 91–97.

Chinchilla, D., Bauer, Z., Regenass, M., Boller, T., and Felix, G. (2006) The Arabidopsis receptor kinase FLS2 binds flg22 and determines the specificity of flagellin perception. *Plant Cell* **18:** 465–476.

Conrath, U., Beckers, G., Flors, V., Garcia-Agustin, P., Jakab, G., Mauch, F., *et al.* (2006) Priming: getting ready for battle. *Mol Plant Microbe Interact* **19:** 1062–1071.

De Almeida, R.F.M., Fedorov, A., and Prieto, M. (2003) Sphingomyelin/phosphatidylcholine/cholesterol phase diagram: boundaries and composition of lipid rafts. *Biophys J* **85:** 2406–2416.

De Vleesschauwer, D., and Hofte, M. (2009) Rhizobacteria-induced systemic resistance. *Adv Bot Res* **51:** 223–281.

Deleu, M., Bouffioux, O., Razafindralambo, H., Paquot, M., Hbid, C., Thonart, P., *et al.* (2003) Interaction of surfactin with membranes: a computational approach. *Langmuir* **19:** 3377–3385.

Dufour, S., Deleu, M., Nott, K., Wathelet, B., Thonart, P., and Paquot, M. (2005) Hemolytic activity of new linear surfactin analogs in relation to their physico-chemical properties. *Biochim Biophys Acta Gen Subj* **1726:** 87–95.

Eeman, A., Francius, G., Dufrene, Y.F., Nott, K., Paquot, A., and Deleu, A. (2009) Effect of cholesterol and fatty acids on the molecular interactions of fengycin with *Stratum corneum* mimicking lipid monolayers. *Langmuir* **25:** 3029–3039.

Eeman, M., Berquand, A., Dufrene, Y.F., Paquot, M., Dufour, S., and Deleu, M. (2006) Penetration of surfactin into phospholipid monolayers: nanoscale interfacial organization. *Langmuir* **22:** 11337–11345.

Felix, G., Regenass, M., and Boller, T. (1993) Specific perception of subnanomolar concentrations of chitin fragments by tomato cells – induction of extracellular alkalinization, changes in protein-phosphorylation, and establishment of a refractory state. *Plant J* **4:** 307–316.

Finking, R., and Marahiel, M.A. (2004) Biosynthesis of nonribosomal peptides. *Annu Rev Microbiol* **58:** 453–488.

Francius, G., Dufour, S., Deleu, M., Papot, M., Mingeot-Leclercq, M.P., and Dufrene, Y.F. (2008) Nanoscale membrane activity of surfactins: influence of geometry, charge and hydrophobicity. *Biochim Biophys Acta Biomembr* **1778:** 2058–2068.

Freudenberg, M.A., Salomao, R., Sing, A., Mitov, I., and Galanos, C. (1998) Reconciling the concepts of endotoxin sensitization and tolerance. *Prog Clin Biol Res* **397:** 261–268.

Grangemard, I., Peypoux, F., Wallach, J., Das, B.C., Labbe, H., Caille, A., *et al.* (1997) Lipopeptides with improved properties: structure by NMR, purification by HPLC and structure–activity relationships of new isoleucyl-rich surfactins. *J Pept Sci* **3:** 145–154.

Heerklotz, H., and Seelig, J. (2001) Detergent-like action of the antibiotic peptide surfactin on lipid membranes. *Biophys J* **81:** 1547–1554.

Heerklotz, H., and Seelig, J. (2007) Leakage and lysis of lipid membranes induced by the lipopeptide surfactin. *Eur Biophys J Biophys Lett* **36:** 305–314.

Huang, X.Q., Lu, Z.X., Zhao, H.Z., Bie, X.M., Lu, F.X., and Yang, S.J. (2006) Antiviral activity of antimicrobial lipopeptide from *Bacillus subtilis* fmbj against Pseudorabies Virus, Porcine Parvovirus, Newcastle Disease Virus and Infectious Bursal Disease Virus *in vitro*. *Int J Pept Res Ther* **12:** 373–377.

Jelokhani-Niaraki, M., Hodges, R.S., Meissner, J.E., Haussenstein, U.E., and Wheaton, L. (2008) Interaction of gramicidin S and its aromatic amino-acid analogs with phospholipid membranes. *Biophys J* **95:** 4494.

Jenny, K., Kappeli, O., and Fiechter, A. (1991) Biosurfactants from *Bacillus licheniformis* – structural analysis and characterization. *Appl Microbiol Biotechnol* **36:** 5–13.

Jones, J.D.G., and Dangl, J.L. (2006) The plant immune system. *Nature* **444:** 323–329.

Jourdan, E., Henry, G., Duby, F., Dommes, J., Barthelemy, J.P., Thonart, P., and Ongena, M. (2009) Insights into the defense-related events occurring in plant cells following perception of surfactin-type lipopeptide from *Bacillus subtilis*. *Mol Plant Microbe Interact* **22:** 456–468.

Kim, S.Y., Kim, J.Y., Kim, S.H., Bae, H.J., Yi, H., Yoon, S.H., *et al*. (2007) Surfactin from *Bacillus subtilis* displays anti-proliferative effect via apoptosis induction, cell cycle arrest and survival signaling suppression. *FEBS Lett* **581:** 865–871.

Kishimoto, K., Kouzai, Y., Kaku, H., Shibuya, N., Minami, E., and Nishizawa, Y. (2010) Perception of the chitin oligosaccharides contributes to disease resistance to blast fungus *Magnaporthe oryzae* in rice. *Plant J* **64:** 343–354.

Kowall, M., Vater, J., Kluge, B., Stein, T., Franke, P., and Ziessow, D. (1998) Separation and characterization of surfactin isoforms produced by *Bacillus subtilis* OKB 105. *J Colloid Interface Sci* **204:** 1–8.

Kracht, M., Rokos, H., Ozel, M., Kowall, M., Pauli, G., and Vater, J. (1999) Antiviral and hemolytic activities of surfactin isoforms and their methyl ester derivatives. *J Antibiot* **52:** 613–619.

Kunze, G., Zipfel, C., Robatzek, S., Niehaus, K., Boller, T., and Felix, G. (2004) The N-terminus of bacterial elongation factor Tu elicits innate immunity in *Arabidopsis* plants. *Plant Cell* **16:** 3496–3507.

Lokossou, A.A., Park, T.H., van Arkel, G., Arens, M., Ruyter-Spira, C., Morales, J., *et al*. (2009) Exploiting knowledge of R/Avr genes to rapidly clone a new LZ-NBS-LRR family of late blight resistance genes from potato linkage group IV. *Mol Plant Microbe Interact* **22:** 630–641.

van Loon, L.C., Bakker, P., van der Heijdt, W.H.W., Wendehenne, D., and Pugin, A. (2008) Early responses of tobacco suspension cells to rhizobacterial elicitors of induced systemic resistance. *Mol Plant Microbe Interact* **21:** 1609–1621.

McHale, L., Tan, X.P., Koehl, P., and Michelmore, R.W. (2006) Plant NBS-LRR proteins: adaptable guards. *Genome Biol* **7:** 212.

Maget-dana, R., and Peypoux, F. (1994) Iturins, a special-class for pore forming lipopeptides – biological and physicochemical properties. *Toxicology* **87:** 151–174.

Maula, T., Westerlund, B., and Slotte, J.P. (2009) Differential ability of cholesterol-enriched and gel phase domains to resist benzyl alcohol-induced fluidization in multilamellar lipid vesicles. *Biochim Biophys Acta Biomembr* **1788:** 2454–2461.

Morikawa, M., Hirata, Y., and Imanaka, T. (2000) A study on the structure–function relationship of lipopeptide biosurfactants. *Biochim Biophys Acta Mol Cell Biol Lipids* **1488:** 211–218.

Naito, K., Taguchi, F., Suzuki, T., Inagaki, Y., Toyoda, K., Shiraishi, T., and Ichinose, Y. (2008) Amino acid sequence of bacterial microbe-associated molecular pattern flg22 is required for virulence. *Mol Plant Microbe Interact* **21:** 1165–1174.

Nurnberger, T., and Kemmerling, B. (2009) PAMP-triggered basal immunity in plants. *Adv Bot Res* **51:** 1–38.

Ongena, M., and Jacques, P. (2008) *Bacillus* lipopeptides: versatile weapons for plant disease biocontrol. *Trends Microbiol* **16:** 115–125.

Ongena, M., Jourdan, E., Schafer, M., Kech, C., Budzikiewicz, H., Luxen, A., and Thonart, P. (2005) Isolation of an n-alkylated benzylamine derivative from *Pseudomonas putida* BTP1 as elicitor of induced systemic resistance in bean. *Mol Plant Microbe Interact* **18:** 562–569.

Ongena, M., Jourdan, E., Adam, A., Paquot, M., Brans, A., Joris, B., *et al*. (2007) Surfactin and fengycin lipopeptides of *Bacillus subtilis* as elicitors of induced systemic resistance in plants. *Environ Microbiol* **9:** 1084–1090.

Peypoux, F., Bonmatin, J.M., and Wallach, J. (1999) Recent trends in the biochemistry of surfactin. *Appl Microbiol Biotechnol* **51:** 553–563.

Pott, T., Dufourcq, J., and Dufourc, E.J. (1996) Fluid or gel phase lipid bilayers to study peptide membrane interactions? *Eur Biophys J Biophys Lett* **25:** 55–59.

Raaijmakers, J.M., de Bruijn, I., and de Kock, M.J.D. (2006) Cyclic lipopeptide production by plant-associated *Pseudomonas* spp.: diversity, activity, biosynthesis, and regulation. *Mol Plant Microbe Interact* **19:** 699–710.

Raaijmakers, J.M., de Bruijn, I., Nybroe, O., and Ongena, M. (2010) Natural functions of lipopeptides from *Bacillus* and *Pseudomonas*: more than surfactants and antibiotics. *FEMS Microbiol Rev* **34:** 1037–1062.

Shen, H.H., Thomas, R.K., Chen, C.Y., Darton, R.C., Baker, S.C., and Penfold, J. (2009) Aggregation of the naturally occurring lipopeptide, surfactin, at interfaces and in solution: an unusual type of surfactant? *Langmuir* **25:** 4211–4218.

Simons, K., and Vaz, W.L.C. (2004) Model systems, lipid rafts, and cell membranes. *Annu Rev Biophys Biomol Struct* **33:** 269–295.

Stanislas, T., Bouyssie, D., Rossignol, M., Vesa, S., Fromentin, J., Morel, J., *et al*. (2009) Quantitative proteomics reveals a dynamic association of proteins to detergent-resistant membranes upon elicitor signaling in tobacco. *Mol Cell Proteomics* **8:** 2186–2198.

Torres, M.A. (2010) ROS in biotic interactions. *Physiol Plant* **138:** 414–429.

Tran, H., Ficke, A., Asiimwe, T., Hofte, M., and Raaijmakers, J.M. (2007) Role of the cyclic lipopeptide massetolide A in biological control of *Phytophthora infestans* and in colonization of tomato plants by *Pseudomonas fluorescens*. *New Phytol* **175:** 731–742.

Tsan, P., Volpon, L., Besson, F., and Lancelin, J.M. (2007) Structure and dynamics of surfactin studied by NMR in micellar media. *J Am Chem Soc* **129:** 1968–1977.

Varnier, A.L., Sanchez, L., Vatsa, P., Boudesocque, L., Garcia-Brugger, A., Rabenoelina, F., *et al*. (2009) Bacterial rhamnolipids are novel MAMPs conferring resistance to *Botrytis cinerea* in grapevine. *Plant Cell Environ* **32:** 178–193.

Vatsa, P., Sanchez, L., Clement, C., Baillieul, F., and Dorey, S. (2010) Rhamnolipid biosurfactants as new players in animal and plant defense against microbes. *Int J Mol Sci* **11:** 5096–5109.

Vollenbroich, D., Pauli, G., Ozel, M., and Vater, J. (1997) Antimycoplasma properties and application in cell culture of surfactin, a lipopeptide antibiotic from *Bacillus subtilis*. *Appl Environ Microbiol* **63:** 44–49.

Volpon, L., Tsan, P., Majer, Z., Vass, E., Hollosi, M., Noguera, V., *et al.* (2007) NMR structure determination of a synthetic analogue of bacillomycin Lc reveals the strategic role of L-Asn1 in the natural iturinic antibiotics. *Spectrochim Acta A Mol Biomol Spectrosc* **67:** 1374–1381.

Yang, S.M., Tang, F., Gao, M.Q., Krishnan, H.B., and Zhu, H.Y. (2010) R gene-controlled host specificity in the legume-rhizobia symbiosis. *Proc Natl Acad Sci USA* **107:** 18735–18740.

Zipfel, C., and Robatzek, S. (2010) Pathogen-associated molecular pattern-triggered immunity: Veni, Vidi . . . ? *Plant Physiol* **154:** 551–554.

Zipfel, C., Robatzek, S., Navarro, L., Oakeley, E.J., Jones, J.D.G., Felix, G., and Boller, T. (2004) Bacterial disease resistance in Arabidopsis through flagellin perception. *Nature* **428:** 764–767.

Zipfel, C., Kunze, G., Chinchilla, D., Caniard, A., Jones, J.D.G., Boller, T., and Felix, G. (2006) Perception of the bacterial PAMP EF-Tu by the receptor EFR restricts *Agrobacterium*-mediated transformation. *Cell* **125:** 749–760.

Supporting information

Additional Supporting Information may be found in the online version of this article:

Supplementary information 1. Cell death not detected in surfactin-treated tobacco cells.
Supplementary information 2. LC-ESI-MS analysis of surfactin derivatives.
Supplementary information 3. Thermodynamic binding model and detailed ITC data.

Please note: Wiley-Blackwell are not responsible for the content or functionality of any supporting materials supplied by the authors. Any queries (other than missing material) should be directed to the corresponding author for the article.